Case Studies in Construction Materials 15 (2021) e00607

Contents lists available at ScienceDirect

Case Studies in Construction Materials

journal homepage: www.elsevier.com/locate/cscm

Case study

Experimental and finite element studies on the behavior of hybrid reinforced concrete beams

Luma Fadhil Hussein [a,*], Mohammed M. Khattab [b], Mustafa Shakir Farman [c]

[a] *Department of Civil Engineering, University of Mustansiriyah, Baghdad, Iraq*
[b] *Institute of Technology, Middle Technical University, Baghdad Iraq*
[c] *Technical Institute of Samawa, Al-Furat Al-Awsat Technical University, Kufa, Iraq*

ARTICLE INFO

Keywords:
Hybrid concrete
Normal reinforced concrete beams
Self-compacting concrete (SCC)
Shear strength

ABSTRACT

This paper presents an experimental and numerical investigation on the behavior of reinforced concrete hybrid beams under two point load. Eight beams of dimensions (150×200×1300 mm) were cast and tested. The hybrid specimens contain of two layers, the upper layer (in the compression zone) made of self-compacted concrete (SCC) with compressive strength of approximately 75 MPa while the layer located in tension zone made of normal strength concrete (NSC) with compressive strength of approximately 30 MPa. These specimens were tested and compared with reference specimens made of SCC or NSC only. The main considered variables were: the SCC layer thickness in hybrid beams; and the effect of shear reinforcement on the total capacity of the tested beams. The test results showed that, using hybrid concrete in casting the reinforced beams has a significant effect in enhancing the general behavior of the specimens. The failure load increased by (18.2–54.5 %) in hybrid beams contained SCC by (25, 50 %) of the total beam height, respectively compared with corresponding reference specimens made of NSC only. It was also noticed that the use of shear reinforcement has an important role in increasing the total capacity of the specimens by about (35.3–38.5 %). ANSYS program (Version 15.0) was employed for modelling the specimens. The numerical results showed that, the general behaviour of the finite element models was in good agreement with the experimental data.

1. Introduction

Reinforced concrete beams are essential structural elements that transfer the load from the slabs to the columns. To perform effectively during its service life, beams must have an adequate safety margin against bending and shear forces. At the ultimate limit state, the combined effects of bending and shear may exceed the shear resistance capacity of the beam causing tensile shear cracks near the support which increased with the increase of applied load and leads to immediate failure of the beam [1].

As a result, in order to achieve high shear strength, superior ductility, and a slight diagonal crack propagation style in any structural member, a high proportion of tensile strength-strain capacity and crack control capability must be achieved. In the last decades, many theoretical and experimental investigations have clarified the influence of several factors such as concrete compressive strength, the

Abbreviations: ACI, American Concrete Institute; ASTM, American Society for Testing and Materials; ANSYS, ANalysis SYStem; HWRA, High Water Reducing Agent; NSC, Normal Concrete Strength; SCC, Self-Compacting Concrete.

* Corresponding author.
E-mail address: luma_civil@uomustansiriyah.edu.iq (L.F. Hussein).

https://doi.org/10.1016/j.cscm.2021.e00607
Received 1 February 2021; Received in revised form 20 May 2021; Accepted 25 June 2021
Available online 29 June 2021
2214-5095/

Nomenclatures

$f_c^{'}$	Specified compressive strength of concrete at 28 days age, MPa
f_y	Specified yield strength of nonprestressing tensile steel, MPa
f_t	Concrete splitting tensile strength, MPa at 28 days age, MPa
f_r	Modulus of rupture of concrete at 28 days age, MPa
E_c	Modulus of elasticity of concrete at 28 days age, MPa
βc	Shear transfer coefficient for a closed crack
βo	Shear transfer coefficient for an open crack
β_1	Factor relating depth of equivalent rectangular compressive stress block to neutral axis depth

existence of shear reinforcement and using fiber reinforced concrete on the total capacity of reinforced concrete beams. Previous researchers [2–5] reported that using enhanced quality materials such as high strength concrete, reactive powder concrete or self-compacting concrete has a significant impact on the enhancement of the shear capacity in reinforced concrete beams. Others [6–8] stated that the use of shear reinforcement gave better shear cracking behavior and effectively enhanced the shear strength. Furthermore, due to the bridging effect of fibers through diagonal cracks, it was found that the shear strength of fiber reinforced concrete increases significantly [9–12]. Fibers are able to dominate crack width and spacing by preventing the opening and growing of diagonal cracks, which substantially advancing aggregate interlock act and dowel act [13–17].

Engineers have recently found hybrid reinforced concrete systems to be of great interest due to their cost-effectiveness and good load-bearing capacity. The definition of hybrid material is not a new idea. Previous researchers [18–20] have described a hybrid girder as one that has either the tension flange or both flanges by using steel section made with a high strength steel grade than the web. Others [21–23] described hybrid reinforced concrete structures as structural elements containing more than one type of reinforcement. While other researchers [24–26] define the hybrid concrete construction as a method of construction which integrates two types of concrete in order to make best advantage of their different inherent qualities.

On that basis, the main goal of the research presented in this paper was to investigate the behavior of ordinary and hybrid reinforced concrete beams with and without shear reinforcement under two point load conditions experimentally and numerically. Also, the study researched the effectiveness of the combination of high-strength self compacted concrete (SCC) and normal strength concrete (NSC) in improving the load capacity of such beams. Normally, the inclined shear cracks start near the support at approximately 45° and extend toward the compression zone of the beam. Shear in cracked reinforced concrete beams is resisted by the flexural compression zone, shear reinforcement and aggregate interlock [27]. So, in hybrid specimens studied in this investigation, the high strength SCC layer placed in the compression zone in order to study its effect in enhancing the total capacity of the tested beams, while NSC layer placed in the tension zone of the tested hybrid beams. The thickness of high strength SCC layer was 100 mm (50 % of the total beam height) and 50 mm (25 % of the total beam height). Also, the results of hybrid specimens were compared with reference specimens made of one type of concrete (either NSC or SCC).

Self compacted concrete provides advantages over vibrated concrete due to its liquid nature; additionally, it is effectively eliminating voids and segregation, reducing the noise level in construction, speeding the process of construction, and improving the quality and ductility of the concrete members. Also, SCC achieves the ability to fill all voids in the formwork and passes through reinforcing bars by its own weight; therefore, vibration is not needed and, as a result, labor is reduced. Additionally, the regularity of microstructure and self-consolidating of SCC reduce the weakened locations in concrete, so it may lead to increased shear strength [11, 28–32].

2. Experimental procedure

2.1. Materials

The materials that were used in this investigation represented by ordinary Portland cement (OPC) with Blaine fineness of 3900 cm^2/g conforming to ASTM C150 [33], crushed coarse aggregate with a maximum size of 10 mm and fine sand passing through 4.75 mm sieve opening size with water absorption and specific gravity of about 2.2 and 2.6, respectively. To produce self-compacting concrete, a superplasticizer known as (High Water Reducing Agent HWRA) based on polycarboxylic ether was used which is free from chlorides and complies with ASTM C494 [34] types A and F. In order to produce high strength concrete, the mixture contain micro silica with specific gravity of 2.32 and pozzolanic activity index of 124.56, which represent the ability of silica (SiO_2) to react with calcium hydroxide (CH), in the presence of water at ordinary temperature to form calcium silicate hydrates (C-S-H) that binds the

Table 1
Mix design.

Type of Concrete	Cement, kg/m^3	Sand, kg/m^3	Gravel, kg/m^3	Water, L/m^3	Silica Fume, kg/m^3	Super-plasticizer, (L/m^3)
NSC	400	600	1200	200	–	–
SCC	557	888	764	170	55.7	17

aggregates and give additional strength to concrete [35]. Table 1 shows the mix design for normal strength concrete (NSC) and self compacted concrete (SCC) mixes.

The flexural reinforcement was 4 Ø12 mm, with yield strength of 350 MPa, placed in the tension zone of the beam. In specimens with shear reinforcement, stirrups of Ø6 @ 50 mm c/c, with yield strength of 620 MPa, was used. The reinforcement in compression zone consisted of 2 Ø8 mm, with yield strength of 480 MPa. Each result of the steel yield strength represent the average of three specimens and the test was performed according to ASTM A370 [36]. In each beam, the cover was equal to 40 mm, Fig. 1 shows the details of reinforcement.

In hybrid concrete specimens, the concrete was placed into molds in two layers. The layer in the bottom of the mold was normal strength concrete and the upper layer was self compacted concrete, which was applied in the mold 30 min after placing normal strength concrete; which is the time of initial setting of cement used in this investigation determined by Vicat's apparatus test, in order to prevent the mixing of the two layers. The beams were de-molded after 24 h and tested after 28 days of curing in tap water. Table 2 shows the characteristics of the tested beams.

2.2. Investigation items

The mechanical properties of normal strength concrete and self compacted concrete mix are determined. The compressive strength, tensile strength, and modulus of elasticity of NSC and SCC were determined using cylindrical specimens with dimensions of 100 mm diameter x 200 mm height according to ASTM C39 [37], ASTM C496 [38] and ASTM C 469-02 [39], respectively. While the flexural strength of concrete was tested by using prisms with a size of 100 mm × 100 mm × 400 mm in accordance to ASTM C78 [40]. Table 3 shows the test results for the above parameters for each beam, while Fig. 2 shows the testing setup of the above items.

Moreover, eight beams of dimensions 150 × 200 × 1300 mm were cast and cured as mentioned above. After 28 days of curing, the specimens were dried at room temperature for 24 h before being painted with a white color, so that cracks can be easily detected. To prevent the beam from developing significant axial forces, which could create artificial strut action, the beams were supported by a roller on one end and a hinge at the other. Every beam was tested by gradually increasing the load until failure under the action of two point loads applied by a Universal testing machine with a capacity of 3000 kN and a loading rate of 5 kN per minute. To record midspan deflection, a dial gauge with 0.002 mm accuracy was tightly fixed to the bottom face of midspan. At each 5 kN load increment, the midspan deflection was measured.

3. Results and discussion

3.1. Load-deflection relationships

For each (5 K N) load increment, vertical deflection in the mid-span of the beam's tension face was measured using a dial gage of sensitivity (0.01 mm). The last deflection reading was always taken prior to the last load increment, which is caused the failure. The load-deflection relationships for the beam specimens are shown in Fig. 3. The following results can be taken from these curves:

- The slope of the curves, at the beginning, is almost identical for all the beams since it depends on the stiffness of the beam.
- For all specimens, the first crack occurs at the same load level.
- After the formation of first crack, the deflection increases until failure associated with an increase in the number of cracks.
- It is clear that the use of hybrid concrete in casting the specimens had a significant effect in improving the behavior of the beams tested under two-point load conditions, i.e. the ultimate load in hybrid concrete beams (HB25, HRB25) were higher than that in

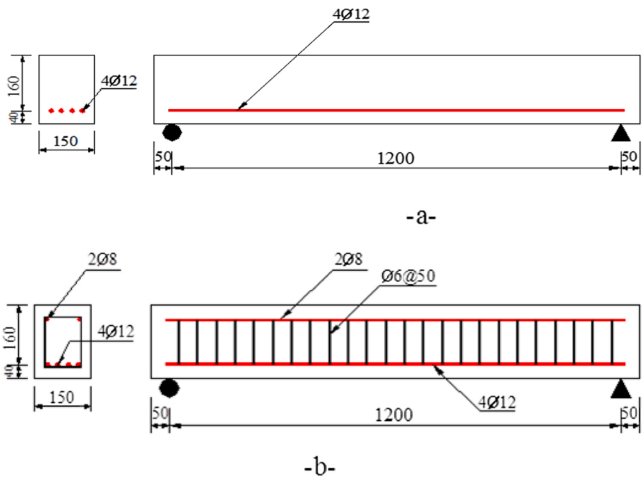

Fig. 1. Reinforcement details (a) for beams without stirrups, (b) for beams with stirrups (all dimensions are in mm).

Table 2
Characteristics of the tested beams.

Beam ID	Type of Concrete	Thickness of SCC Layer (% of total beam height)	Thickness of SCC Layer, mm	Shear Reinforcement
NB	NSC	0	0	–
HB50	Hybrid (NSC and SCC)	50	100	–
HB25	Hybrid (NSC and SCC)	25	50	–
SCB	SCC	100	200	–
NRB	NSC	0	0	Ø6 @ 50 mm c/c
HRB50	Hybrid (NSC and SCC)	50	100	Ø6 @ 50 mm c/c
HRB25	Hybrid (NSC and SCC)	25	50	Ø6 @ 50 mm c/c
SRCB	SCC	100	200	Ø6 @ 50 mm c/c

Table 3
Results of plain concrete tests.

Beam ID	Type of concrete	Compressive strength f'_c, (MPa)	Splitting tensile strength f_t, (MPa)	Flexural strength f_r, (MPa)	Modulus of elasticity E_c, (MPa)
NB	**NSC**	26.20	3.00	3.45	25101
HB50	**NSC**	27.80	3.22	3.30	24400
	SCC	73.50	4.50	4.91	34189
HB25	**NSC**	25.80	3.07	3.78	25200
	SCC	77.20	4.67	5.41	35000
SCB	**SCC**	75.50	4.75	5.38	33521
NRB	**NSC**	27.50	3.2	3.67	24200
HRB50	**NSC**	26.46	3.14	3.19	25673
	SCC	74.20	4.78	5.61	32780
HRB25	**NSC**	28.00	3.34	3.54	24899
	SCC	75.60	4.39	5.33	33400
SRC	**SCC**	73.03	4.32	5.58	34041
Standard	**NSC**	1.000	0.116	0.203	22712.47
Deviation	**SCC**	1.414	0.179	0.264	30959.76

Note: Each result of the mechanical properties represents the average of three specimens.

beams (NB, NRB), respectively. While this increase was very clear in specimens (HB50, HRB50) due to the increase in the thickness of high strength SCC layer.

- It was revealed that the trend of load-deflection curves of hybrid beams (HB50, HRB50) was similar to the specimens (SCB, SRCB) respectively.
- The deflection values in hybrid beams were smaller than those in normal concrete beams at the same load level.
- The inclusion of shear reinforcement improves the total capacity of the tested specimens significantly. The ductility of these specimens has also been increased, as shown by the long extension of the diagrams of these specimens.

3.2. *Cracking and deformability of the tested specimens*

Table 4 shows the magnitude of the cracking load and the related deflection for the tested specimens at the beam's mid span.

It is clear that the existence of hybrid concrete has no impact on the cracking load value. The effect of shear reinforcement, on the other hand, had a major influence on the specimens' general behavior; the cracking load in specimens reinforced with stirrups was about 35 % higher than that in corresponding specimens without shear reinforcement.

3.3. *Load carrying capacity for the tested specimens*

The values of failure load for all experimental specimens are shown in Table 5. Based on this data, it can be concluded that using SCC in hybrid beams by (25, 50 %) of the total beam height resulted in increasing the failure load by (18.2–54.5 %), respectively compared with reference specimens (made with NSC). However, the values of ultimate load for the specimens made of SCC only (SCB and SRCB) are higher than that of hybrid concrete. Hence, the use of high strength concrete enhanced the performance of the beams.

It is worthy to mention that, in comparison to the reference specimens without stirrups, the use of shear reinforcement has a significant effect in increasing the total capacity of the specimens by about (35.3–38.5 %).

3.4. *Crack pattern*

The crack patterns of the tested beams are shown in Fig. 4. It is clear that, the use of stirrups change the mode of failure from pure shear in beams without stirrups to shear-flexure failure in beams reinforced with stirrups. Also, the cracks seem to be finer and higher in number in hybrid beams compared with beams made of one layer, this indicates that the use of hybrid concrete enhanced the general

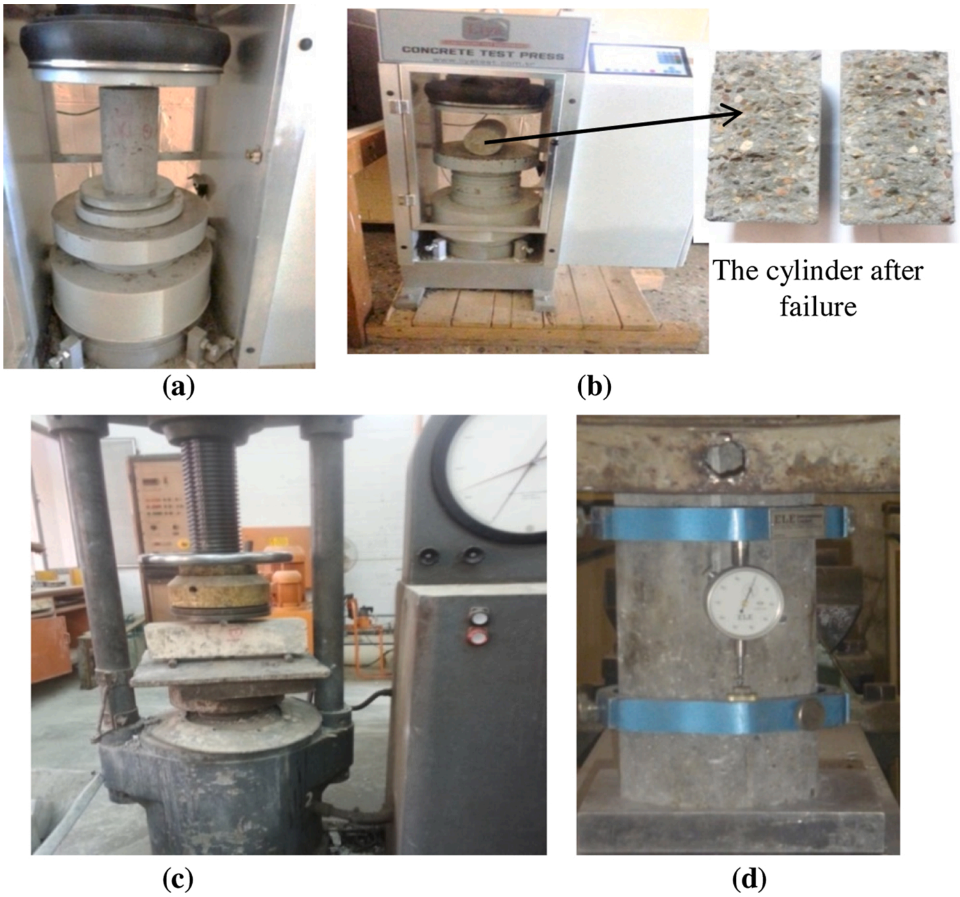

Fig. 2. Testing setup for, (a) Compressive strength, (b) Splitting tensile strength, (c) Flexural strength and (d) Modulus of elasticity.

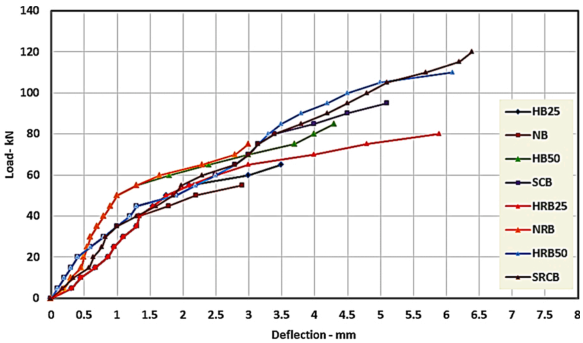

Fig. 3. Load - deflection relationships for beams specimens.

behaviour of the beams.

4. Finite element formulation

Numerical methods such as finite element and finite difference have been used in a much more realistic way to achieve approximate solutions to complex problems. In this study, the specimens were modelled and analysed using ANSYS computer program (version 15) in order to show the agreement between experimental work and numerical analysis. The results are compared with experimental results including the ultimate load, ultimate deflection and crack pattern.

The idealization of reinforced concrete members by using finite element method must be able to represent concrete cracking, crushing, the interaction between concrete and reinforcement, and the ability of concrete to transmit shear by aggregate interlocking

Table 4
First crack load and deflection results of the tested beam Specimens.

Beam ID	First crack load, (kN)	First crack deflection, (mm)
NB	15	0.58
HB25	15	0.46
HB50	15	0.67
SCB	20	0.40
NRB	20	0.48
HRB25	20	0.87
HRB50	20	0.40
SRCB	27	0.77

Table 5
Ultimate failure load and corresponding deflection results for the tested beam specimens.

Beam ID	Failure load, kN	***IRL***, %	***IRS***, %	Ultimate deflection, mm
NB	55	–	–	2.9
HB25	65	18.2	–	4.3
HB50	85	54.5	–	3.5
SCB	95	72.7	–	5.1
NRB	75	–	36.4	3
HRB25	90	20.0	38.5	6.5
HRB50	115	53.3	35.3	6.5
SRCB	130	73.3	36.8	7.0

Note: IRL = increasing ratio of failure load depending on the thickness of SCC layer; IRS = increasing ratio of failure load due to the existence of shear reinforcement (stirrups).

after cracking. In the current study, an 8-node three-dimensional brick element (SOLID-65 in ANSYS) was used to model the concrete.

The steel reinforcements, on the other hand, were represented using 2-node discrete representation (LINK-180 in ANSYS) and included in the properties of 8-node brick elements. It is assumed that the reinforcement can only transmit axial forces, and it is assumed that there is a perfect bond between the concrete and the reinforcing bars. The link element for the steel reinforcing bar was connected between nodes of each adjacent concrete solid element in order to provide the perfect bond, so that the two materials share the same nodes. In addition, the support was represented using 8-node (Solid-185 in ANSYS) three-dimensional brick component.

4.1. Material properties of the beams models

Parameters needed to define the material properties for the models are given in Table 6. As seen in this table, there are multiple parts of the material properties for each element. To properly modulate the concrete, the brick component SOLID65 requires linear isotropic (concrete elasticity unit, E_c and Poisson's ratio of concrete PRXY) and multi-linear isotropic material properties.

For flexural reinforcement, secondary reinforcement and stirrups, the LINK 180 element was used. Bilinear isotropic material was assumed which represented by the steel elasticity unit (E_s) and the PRXY parameter that reflects the steel Poisson's ratio, which is tacked as (0.3). Von Mises' failure criterion also follows the bilinear model and allows the yield stress (f_y) as well as the steel's hardening module to be established. It is assumed that their hardening module (tangent module) is zero.

After specifying the volumes and the reinforcement, the next step of the finite element analysis requires creating the meshing of the model. Before meshing, all the lines are divided into segments of 25 mm length. For concrete, a rectangular mesh with hexahedron (brick) volume is recommended for meshing the specimens using SOLID 65 element. For the displacement boundary conditions, the beam was modeled to be simply supported. The load was applied in the same way as it was in the experimental work, see Fig. 5.

5. Comparison between numerical and experimental models

5.1. Load – deflection response

Fig. 6 shows the experimental and numerical load-deflection curves at mid span of each model. It can be noted that there is a good agreement between the results of the finite element model and the experimental performance of these specimens. At the linear stage, however, the finite element load-deflection curves are somewhat stiffer than the experimental responses for tested beams. The stiffness of the modelled beams is slightly higher after the formation of first crack compared to that of the experimental specimens. There are several reasons why the finite element models can be extremely rigid. First micro-cracks created by drying shrinkage and handling that are present in concrete to some degree will reduce the rigidity of the actual samples, while the models of finite elements do not include micro-cracks. Second, in the finite element analysis, the perfect bond between concrete and reinforced steel is assumed, this assumption would not be true for the actual samples. Also, the composite action between concrete and reinforcing steel in experimental specimens starts to decrease as bond slip occurs. Thus, the overall rigidity of the actual specimens could be lower than that predicted by

Fig. 4. Crack pattern for the tested beams.

the finite element models due to factors that are not included in the models.

On the other hand, by comparing the experimental and numerical values of ultimate load and deflection at mid span of each specimen which is illustrated in Table 7, it was found that the discrepancy ratio of mid-span deflection was about (9.2–30.3 %). These values can be considered acceptable and it could be explained that the main reason may from the ANSYS software which consider full interaction between concrete materials and steel rebar, where this assumption may not be true at the experimental work. Also, may from the experimental procedure which includes load and deformation recording or the actual concrete and steel strengths. Fig. 7 shows the numerical deflected shape of some models at failure.

Table 6
Material properties for the models.

Material	Element	Material Properties			Material	Element	Material Properties		
		Linear Isotropic					Linear Isotropic		
		E_c (MPa)	25101				E_c (MPa)	33521	
		PRXY	0.2				PRXY	0.2	
		Multi-Linear Isotropic					Multi-Linear Isotropic		
		Point No.	Stress MPa	Strain	Self Compacting Concrete	Solid 65	Point No.	Stress MPa	Strain
		1	8.034	0.0003			1	9.9	0.0003
Normal Strength Concrete	Solid 65	2	14.96	0.0006			2	19.8	0.0006
		3	23.64	0.0009			3	29.7	0.0009
		4	26.2	0.002			4	50.33	0.002
		5	26.2	0.003			5	64.3	0.003
		Concrete					Concrete		
		β_o		0.6			β_o		0.6
		β_c		0.9			β_c		0.9
		f_{ct}		3.0 MPa			f_{ct}		7.5 MPa
		f'_c		30 MPa			f'_c		75 MPa
		Linear Isotropic			Secondary reinforcement	Link 180 (Ø8 mm)	Linear Isotropic		
Main reinforcement (flexural reinforcement)	Link 180 (Ø12 mm)	E_s (MPa)		200000			Es (MPa)		200000
		PRXY		0.3			PRXY		0.3
		Bi-Linear Isotropic					Bi-Linear Isotropic		
		Yield Stress (MPa)		350			Yield Stress (MPa)		480
		Tang Mod. (MPa)		0			Tang Mod. (MPa)		0
		Linear Isotropic			Support	Solid 185	Linear Isotropic		
		E_s (MPa)		200000			Es (MPa)		2000000
Stirrups	Link 180 (Ø6 mm)	PRXY		0.3			PRXY		0.3
		Bi-Linear Isotropic							
		Yield Stress (MPa)		620					
		Tang Mod. (MPa)		0					

Note: βo is the coefficient of shear transfer for an open crack; βc is the coefficient of shear transfer for a closed crack; f_{ct} is the cracking stress of uniaxial tensile; f'_c is the crushing uniaxial pressure.

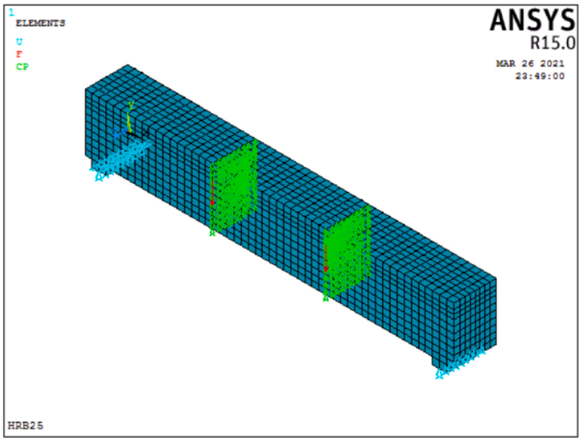

Fig. 5. Meshing, loading and displacement boundary conditions for studied specimens.

5.2. Cracking and ultimate loads of the modelled specimens

The load was applied in steps in each model as it was done in experimental work. The ultimate load for the finite element model is taken from the last applied load step before the solution divergence due to numerous cracks and large deflections. Table 8 provides a comparison of the cracking results with the ultimate loads between the experimental beams and the models of finite elements. From Table 8, it was found that the ANSYS models underestimate the failure load. That is attributed to toughening mechanism at the crack faces. So, once a crack is formed, no tension force perpendicular to the crack can be transmitted across it. However, as long as the crack is narrow, it can still transmit forces in its own plane through interlocking of the surface roughness. Accordingly, the grain bridging and interlocking process between the cracked surfaces may slightly delay the collapse of the experimental specimens, where the finite

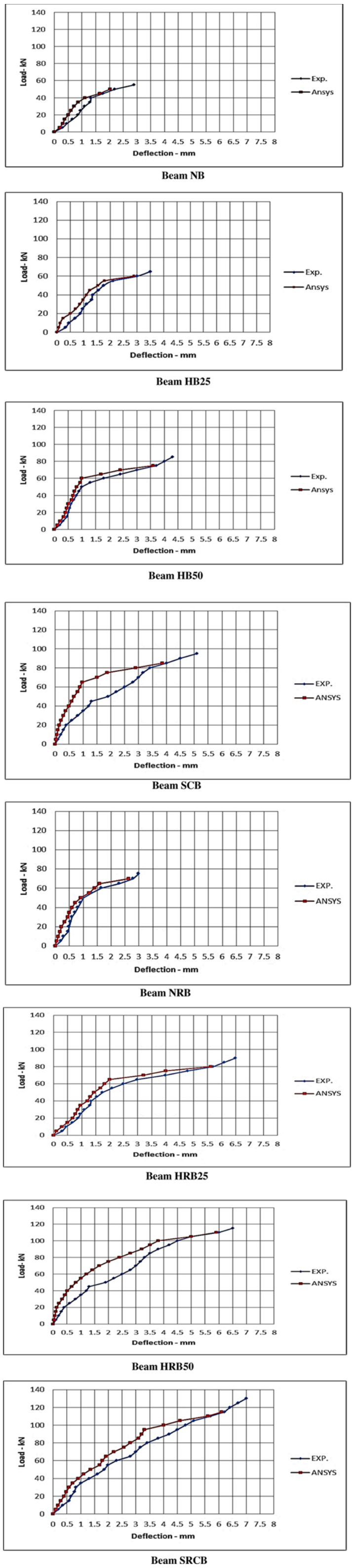

Fig. 6. Experimental and numerical load-deflection curves at mid span of each model.

Table 7
Experimental and numerical results of mid-span deflection.

Beam ID	Ultimate load, (kN)			Mid-span deflection, (mm)		
	Exp.	ANSYS	Discrepancy, %	Exp.	ANSYS	Discrepancy,%
NB	55	50	10.0	2.9	2.02	30.3
HB25	65	60	7.7	3.5	2.9	17.1
HB50	85	75	11.8	4.3	3.6	16.3
SCB	95	85	10.5	5.1	3.86	24.3
NRB	75	70	6.7	3	2.62	12.7
HRB25	90	83	7.8	6.5	5.6	13.8
HRB50	115	109	5.2	6.5	5.9	9.2
SRCB	130	115	11.6	7.0	6.1	12.8

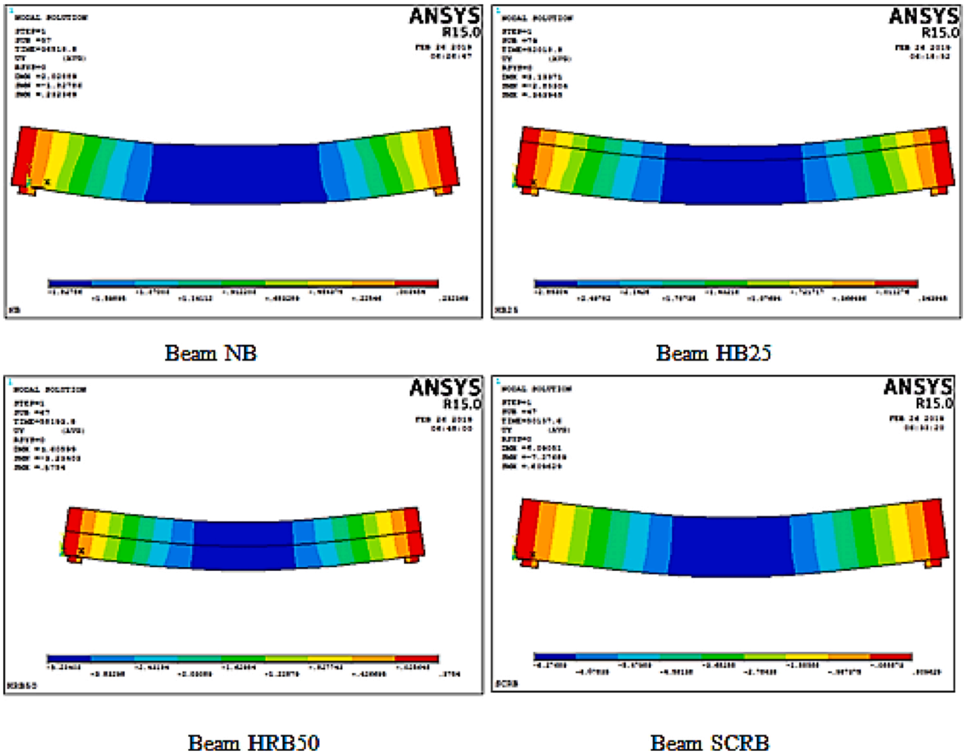

Fig. 7. Numerical deflected shape of some models at failure.

Table 8
Experimental and numerical results of cracking and ultimate loads for tested models.

Beam Labelling	Cracking load, (kN)		Ultimate load, (kN)		
	Expi.	ANSYS	Expi.	ANSYS	Discrepancy, %
NB	15	10	55	50	9.1
HB25	15	12	65	60	7.7
HB50	15	13.5	85	75	11.8
SCB	20	17	95	85	10.5
NRB	15	12	75	70	6.7
HRB25	20	16.5	90	83	7.8
HRB50	20	18	115	109	5.2
SRCB	25	23	130	115	11.5

element models ignore these mechanisms.

Based on the numerical results, it was noticed that the use of hybrid concrete has a significant rule in enhancing the total capacity of the models which increased by about (20–30 %) and (18.6–55.7 %) in hybrid beams without and with shear reinforcement, respectively compared with corresponding reference normal strength concrete beam. On the other hand, the use of shear reinforcement has a noticeable effect on the total resistance which was increased by about (35.3–45.3 %) due to the use of stirrups in the modelled beams. Also the discrepancy ratio between experimental and ANSYS results for ultimate load ranged between (5.2–11.8 %). This indicates that the modelling of the specimens was very accurate due to the use of the same concrete properties and the use of hex sweep mesh.

5.3. Crack pattern of the modelled specimens

ANSYS program records the crack pattern at each applied load step. A cracking sign represented by a circle appears when a principal tensile stress exceeds the ultimate tensile strength of the concrete. In all specimens the first crack appears in the tension face of the model at about (16.5–20 %) of the ultimate load. In specimens without shear reinforcement, the first crack appears in the tension face of the beam near the support. While it appears in the tension face at mid span of the beams reinforced with shear reinforcement. As the load increased, the cracks increased in number and extend towards the upper side of the beam. This behaviour is similar to that observed during the experimental work. Also, it was found that the number of cracks in hybrid beams were lower than that in normal strength concrete specimens.

Besides, the existence of shear reinforcement played a good rule in increasing the total stiffness of the model and as a result the total number of cracks decreased.

6. Conclusions

The following conclusions can be established from the test and numerical results obtained in this study:

- The existence of hybrid concrete has no impact on the cracking load value. On the other hand, the cracking load in specimens reinforced with stirrups was about 35 % higher than that in corresponding specimens without shear reinforcement.
- Using SCC in hybrid beams by (25, 50 %) of the total beam height resulted in increasing the failure load by (18.2–54.5 %), respectively compared with reference specimens (made with NSC). Hence, the use of high strength concrete enhanced the performance of the beams.
- By comparing the specimens reinforced with stirrups with those without shear reinforcement, it was found that the ultimate load increased by about (35.3–38.5 %). This indicates that the existence of shear reinforcement had a significant effect in enhancing the ductility and total capacity of the tested specimens.
- The use of stirrups change the mode of failure from pure shear in beams without stirrups to shear-flexure failure in beams reinforced with stirrups. Also, the cracks seem to be finer and higher in number in hybrid beams compared with beams made of NSC or SCC, this indicates that the use of hybrid concrete enhanced the general behaviour of the beams.
- By comparing the experimental and numerical values of ultimate load and deflection at mid span of each specimen, it was found that the discrepancy ratio between experimental and ANSYS results for ultimate load and deflection ranged between (5.2–11.8 %) and (9.2–30.3 %), respectively. This indicates that the modelling of the specimens was very accurate due to the use of the same concrete properties and the use of hex sweep mesh.

Declaration of Competing Interest

The authors declare that they have no conflict of interest.

Acknowledgments

The authors would like to thank Mustansiriyah University (www.uomustansiriyah.edu.iq) Baghdad – Iraq for its support in the present work.

References

[1] M. Khuntia, B. Stojadinovic, Shear strength of reinforced concrete beams without transverse reinforcement, ACI Struct. J. 98 (5) (2001) 648–656.
[2] M. Ridhaa, S. Kaiss, A. Ihsan, Experimental study and shear strength prediction for reactive powder concrete beams, Case Stud. Constr. Mater. 8 (2018) 434–446.
[3] F. Libin, Shear Enhancement in Reinforced Concrete Beams, Ph.D. Thesis, Imperial College London, London, 2014, p. 310.
[4] A.M.T. Hassan, S.W. Jones, G.H. Mahmud, Experimental test methods to determine the uniaxial tensile and compressive behavior of ultra-high performance fiber reinforced concrete (UHPFRC), Const. Build. Mater. J. 37 (2012) 874–882.
[5] J. Hegger, D. Tuchlinshi, B. Kommer, Bond anchorage behavior and shear capacity of ultra-high performance concrete beams, in: Proc. Int. Symp. on Ultrahigh Performance Concrete, ASCE Reston, 2004, pp. 351–360.
[6] J.Y. Lee, U.Y. Kim, Effect of longitudinal tensile reinforcement ratio and shear span-depth ratio on minimum shear reinforcement in beams, ACI Struct. J. 105 (2) (2008) 44–134.
[7] E.J. Tompos, R.J. Frosch, Influence of beam size, longitudinal reinforcement, and stirrup effectiveness on concrete shear strength, ACI Struct. J. 99 (5) (2002) 59–67.
[8] G. Russo, D. Mitri, M. Pauletta, Shear strength design formula for RC beams with stirrups, Eng. Struct. J. 51 (2013) 226–235.
[9] G. Campione, C. Cucchiara, L. La Mendola, Role of fibres and stirrups on the behaviour of reinforced concrete beams under flexure and shear. Composite in constructions, Cosenza, 2003, pp. 97–102.

[10] M. Nili, V. Afroughsabet, Combined effect of silica fume and steel fibers on the impact resistance and mechanical properties of concrete, Int. J. Impact Eng. 37 (8) (2010) 879–886.
[11] M. Pająk, T. Ponikiewski, Flexural behavior of self-compacting concrete reinforced with different types of steel fibers, Constr. Build. Mater. 47 (2013) 397–408.
[12] P.R. Tadepalli, H.B. Dhonde, Y. Mo, T.T. Hsu, Shear strength of prestressed steel fiber concrete I-beams, Int. J. Concr. Struct. Mater. 9 (3) (2015) 267–281.
[13] E. Shehata, Fiber-reinforced Polymer (FRP) for Shear Reinforcement in Concrete Structures, PhD Thesis, University of Manitoba, Winnipeg, Canada, 1999.
[14] Z. Omeman, M. Nehdi, H. El-Chabib, Experimental study on shear behavior of CFRP-reinforced concrete short beams without web reinforcement, Am. J. Civ. Eng. 35 (1) (2008) 1–10.
[15] B. Srudhira, M. Anil kumar, K.J. Brahma Chari, Evaluation of shear behaviour of RC beams using CFRP, Int. J. Recent Technol. Eng. (IJRTE) 7 (6) (2019).
[16] N. Spinella, Shear strength of full-scale steel fibre-reinforced concrete beams without stirrups, Comput. Concr. 11 (5) (2013) 365–382.
[17] M.M. Kamal, M.A. Safan, Z.A. Etman, R.A. Salama, Behavior and strength of beams cast with ultra-high strength concrete containing different types of fibers, HBRC J. 10 (2014) 55–63.
[18] U. Fathoni, H. Norhasniyati Mat, Flexural behaviour of hybrid concrete beam, in: the 3rd National Graduate Conference (NatGrad2015), University Tenaga Nasional, Putrajaya Campus, 2015.
[19] S. Mehdi, S. Yongjiu, Flexural strength of hybrid steel I-beams based on slenderness, J. Eng. Struct. 93 (2015) 114–128.
[20] C.R. Earley, M.A. AbeolSeoud, J.J. Myers, Early-age behavior and construction sequencing of hybrid composite beam (HCB) bridges in Missouri, USA, in: 11th International Symposium on Fiber Reinforced Polymer for Reinforced Concrete Structures, Guimarães, Portugal, 2013.
[21] M. Barzin, Y. Yiming, S. Chote, Analytical solutions for flexural design of hybrid steel fiber reinforced concrete beams, J. Eng. Struct. 100 (2015) 164–177.
[22] K. Habel, Structural Behavior of Elements Combining Ultra-high Performance Fiber Reinforced Concretes (UHPFRC) and Reinforced Concrete, Ph.D. Thesis, Ecole Polytechnique Federal De Lausanne, Switzerland, 2004, p. 195.
[23] M.A. EDER, Inelastic Behaviour of Hybrid steel/concrete Column-to-flat Slab Assemblages, Ph.D. Thesis, Imperial College London, 2011.
[24] G. Yaarub, T. Hind, Behavior of hybrid reinforced concrete beams combining reactive powder concrete and varying types of lightweight concrete, J. Eng. Dev. 20 (2) (2016) 204–223.
[25] R. Suha, J. Haitham, Behavior of hybrid concrete beams containing two types of high strength concrete (HSC) and conventional concrete, Int. J. Sci. Res. (IJSR) 6 (8) (2017) 708–716.
[26] A.N. Amer, J.M. Ahmed, Torsional behavior of hybrid reinforced concrete box girders composed of conventional concrete and modified reactive powder concrete, Civ. Environ. Res. 9 (10) (2017).
[27] S. Campana, M.F. Ruiz, A. Anastasi, A. Muttoni, Analysis of shear-transfer actions on one-way RC members based on measured cracking pattern and failure kinematics, Mag. Concr. Res. 65 (2013).
[28] L. Biolzi, S. Cattaneo, F. Mola, Bending-shear response of self-consolidating and high-performance reinforced concrete beams, Eng. Struct. 59 (2014) 399–410.
[29] Y. Fritih, T. Vidal, A. Turatsinze, G. Pons, Flexural and shear behavior of steel fiber reinforced SCC beams, KSCE J. Civil. Eng. 17 (6) (2013) 1383–1393.
[30] O. Gensel, W. Brostow, T. Datashvili, M. Thedford, Workability and mechanical performance of steel fiber-reinforced self-compacting concrete with fly ash, Compos. Interfaces 18 (2011) 169–184.
[31] R. Ghavidel, R. Madandoust, M.M. Ranjbar, Reliability of pull-off test for steel fiber reinforced self-compacting concrete, Measurement 73 (2015) 628–639.
[32] N.K. Oukaili, L.F. Hussein, Experimental and analytical study on punching shear strength of BubbleDecks, ACI Struct. J. 117 (2) (2020) 17–31.
[33] ASTM C 150-07, Standard Specification for Portland Cement, Annual Book of ASTM Standards, 04.01, ASTM International, 2009.
[34] ASTM C 494/C 494M, Standard Specification for Chemical Admixtures for Concrete, Annual Book of ASTM Standards, 04.02, ASTM International, 2001.
[35] R.T. Thorstensen, P. Fidjestol, Inconsistencies in the pozzolanic strength activity index (SAI) for silica fume according to EN and ASTM, Mater. Struct./Materiaux et Constructions 48 (12) (2015) 3979–3990.
[36] ASTM A 370-18, Standard Test Methods and Definitions for Mechanical Testing of Steel Products, Annual Book of ASTM Standards, ASTM International, 2018.
[37] ASTM C39/C39M, Standard Test Method for Compressive Strength of Cylindrical Concrete Specimens, American Society for Testing and Materials, United States, 2001.
[38] ASTM C496/C496M, Standard Test Method for Splitting Tensile Strength of Cylindrical Concrete Specimens, American Society for Testing and Materials, United States, 2011.
[39] ASTM C469-02, Standard test method for static modulus of elasticity and Poisson's ratio of concrete in compression. Annual Book of ASTM Standards, American Society for Testing and Material, 2002.
[40] ASTM C.78, Standard Test Method for Flexural Strength of Concrete (Using Simple Beam With Third-point Loading), American Society for Testing and Materials, United States, 2002.